

Energy-Angular Correlations and Sequential Decay in the ${}^2\text{H}(p, 2p)n$ and ${}^1\text{H}(d, 2p)n$ Reactions*

W. D. SIMPSON, J. D. BRONSON,† W. R. JACKSON, G. C. PHILLIPS

Rice University, Houston, Texas

I. INTRODUCTION

The recent development of commercially available multiparameter pulse-height analyzers and of computer-coupled analyzer systems¹ has made it possible to investigate, by coincidence techniques, the energy and angular distributions of two of the nucleons from the breakup of a three-nucleon system. In the present investigation, the reactions ${}^2\text{H}(p, 2p)n$ and ${}^1\text{H}(d, 2p)n$ have been studied by detecting the two breakup protons in coincidence for a number of different laboratory angles and bombarding energies. Earlier results indicating the sequential decay of this three-nucleon system *via* the virtual, singlet deuteron have been presented elsewhere.² Further evidence of the virtual, singlet deuteron is presented here, along with evidence indicating sequential breakup in the ${}^1\text{H}(d, 2p)n$ reaction *via* an intermediate state in the $(p+p)$ system corresponding to the di-proton.

II. KINEMATIC CONSTRAINTS ON THE THREE-PARTICLE SYSTEM

In reactions involving three particles in the final state, nine scalar variables in the center-of-mass system are required to specify completely the system kinematically. We may employ the constraints due to conservation of energy (1 constraint) and momentum (3 constraints) to reduce the number of variables to be determined to five. Thus the system should be completely specified kinematically by measuring or determining five scalar variables, T_1' , θ_1' , θ_2' , Φ_1' , and Φ_2' with the constraints of the system then determining the remaining four variables T_2' , T_3' , θ_3' , and Φ_3' .

However, due to the quadratic dependence of T_2' on T_1' , five scalar variables will not suffice to completely determine the kinematics. Instead we may find some (and perhaps all) values of allowed T_1 (the laboratory energy of the particle detected in counter 1) which correspond to two different values of T_2 (the laboratory energy of the particle detected in the second counter) which we can label as T_2^- and T_2^+ . Thus, in

order to specify completely the system kinematically, we must now also measure T_2 in order to determine which solution of the kinematics (T_2^- or T_2^+) is the valid one for any given coincident event.

In the work discussed here this complete specification was accomplished by two solid-state surface-barrier detectors, both capable of determining charged-particle energies with good resolution, mounted in a reaction chamber specifically built for the study of reactions involving three particles in the final state.³ The coincident pulses from the two detectors were analyzed by a two-parameter pulse-height analyzer; the earlier data were collected with a commercial 32×32 channel analyzer, and the more recent data with the Rice 1000×1000 channel computer-analyzer system. With both systems "accidental" coincident spectra were taken in order to eliminate the effect of any random coincident events which may be recorded with the "true" coincident events of the data.

The recorded array of coincident events falls along some definite, kinematically determined locus in the T_2 versus T_1 plane. The intensity of the distribution of these events along the locus provides a sensitive indication of the process involved in the breakup of the three particle system. Each point on this locus corresponds to a particular internal energy in the systems (2, 3), (1, 3), and (1, 2) which correspond to particles 1, 2, and 3 being the first emitted particles, respectively. These internal energies are easy to calculate, and when plotted along with the data indicate at a glance what internal energies are available for a particular region of the kinematic locus which may be of interest. The usefulness of such plots is discussed further in the presentation of the data.

III. THE EFFECT OF THE AVAILABLE PHASE-SPACE

In interpreting the data obtained from a reaction involving three particles in the final state it is important to allow for effects due entirely to the fact that an observation is being made of a system made all the more complex because the observation must be made in the laboratory rather than in the c.m. system. Of particular interest, then, is how the phase-space available to the reaction will manifest itself in the laboratory. This

* Work supported in part by the U. S. Atomic Energy Commission.

† Present address: The University of Basel, Basel, Switzerland.

¹ A. C. L. Barnard, R. Keyes, J. A. Buchanan, T. A. Rabson, and G. C. Phillips, *Bull. Am. Phys. Soc.* **9**, 488 (1964).

² W. D. Simpson, J. D. Bronson, W. R. Jackson, and G. C. Phillips, *Bull. Am. Phys. Soc.* **9**, 389 (1964); W. D. Simpson, M. A. thesis, Rice University (1963) (unpublished).

³ J. D. Bronson, Jr., Ph.D. thesis, Rice University (1964) (unpublished).

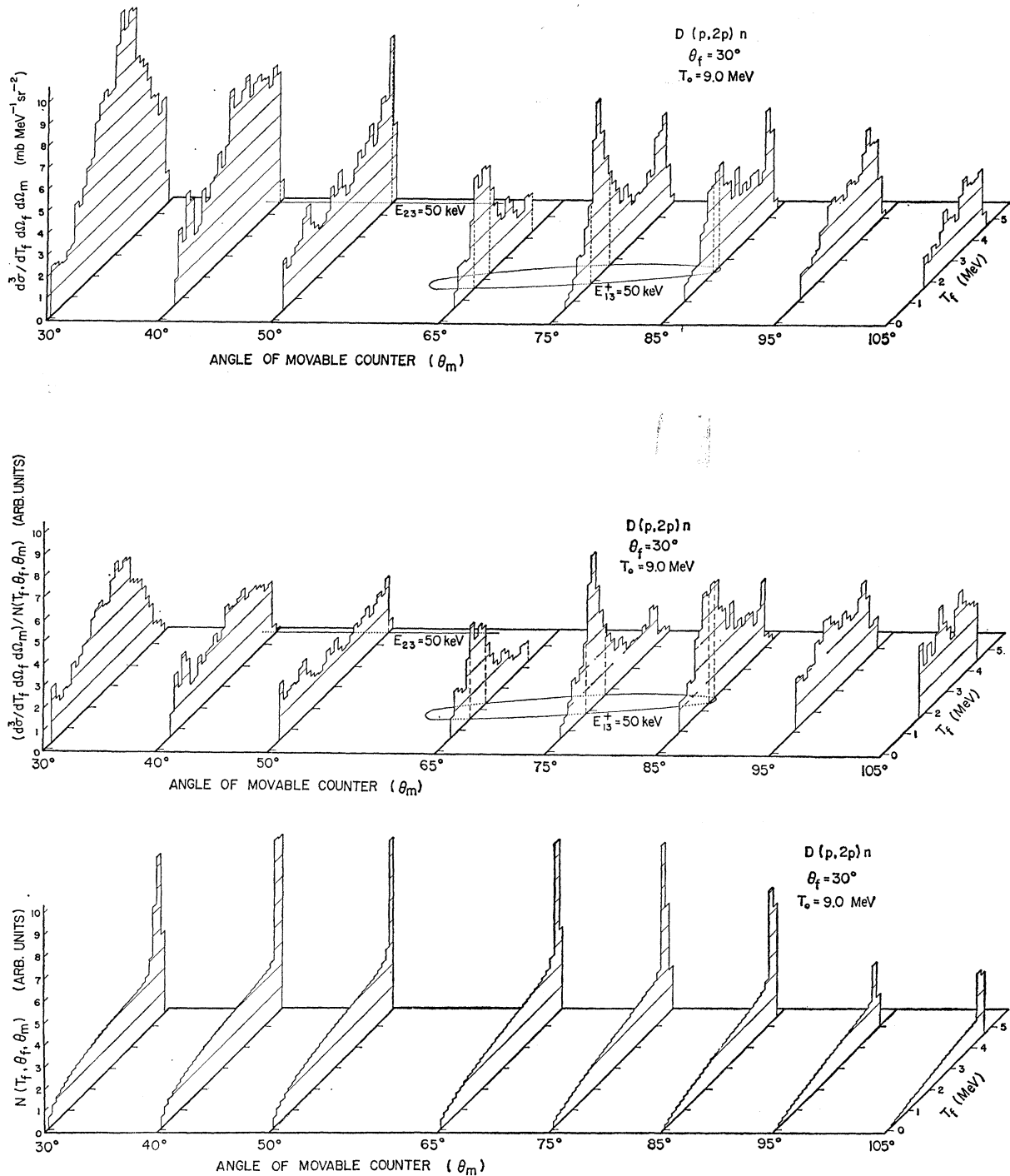


FIG. 1. A three-dimensional, isometric projection of coincident counts for the ${}^2\text{H}(p, 2p)n$ reaction in the $T_{\text{fixed}}, \theta_{\text{moving}}$ plane. The bombarding energy is 9.0 MeV and θ_{fixed} is 30° . The curve E_{23} indicates the locus of events proceeding via a sequential breakup in which the proton detected in the fixed counter (1) is first emitted, leaving the system (2, 3) with 50-keV internal energy. The curve E_{13} indicates the locus of events proceeding via a sequential breakup in which the proton detected in the movable counter (2) is first emitted, leaving the system (1, 3) with 50-keV internal energy. The upper diagram consists of the projected data on the T_f axis for each of the observed angles. Thus the data are presented as the cross section plotted versus the energy of the proton detected in the fixed counter and versus the angle of the movable counter. The center diagram is a similar display, but presented as the ratio of the observed yield to the available phase-space. The lower diagram indicates this available phase-space, i.e., the distribution expected if the reaction were to proceed via simultaneous emission and with intensity proportional to the phase-space available.

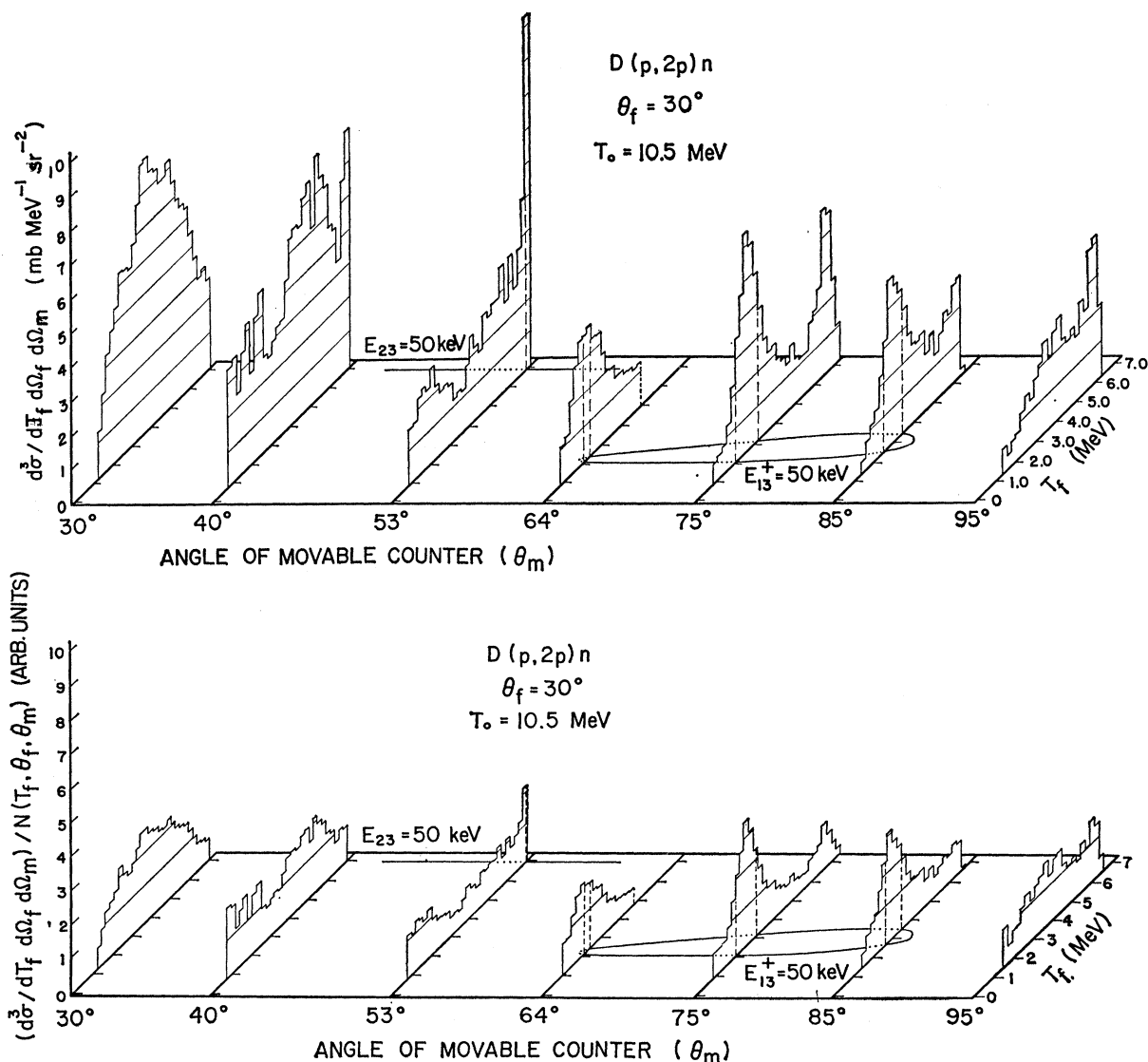


FIG. 2. A three-dimensional, isometric projection of coincident events for the ${}^2\text{H}(p, 2p)n$ reaction in the $T_{\text{fixed}}, \theta_{\text{moving}}$ plane (see Fig. 1). The bombarding energy in this case is 10.5 MeV and θ_{fixed} is 30° . The upper diagram consists of the collected data presented as cross section versus T_f versus θ_m , while the lower diagram is the ratio of this yield to the available phase-space.

subject has been discussed in detail by other authors,⁴ and only a brief description will be given here.

Suppose that for simultaneous three-body breakup that the breakup distribution is proportional to the volume of available phase-space. We wish to determine the probability of finding particle 1, which has emerged in the solid angle Ω_1 , with a momentum between p_1 and $p_1 + dp_1$ when particle 2 has emerged in the solid angle Ω_2 . Thus we wish to compute the distribution function $N(p_1, \Omega_1, \Omega_2)$ for the case of three-body planar breakup.

The total integrated yield over all angles and momenta will be proportional to N_T , defined as:

$$N_T = \int_{i=1,3}^{p_i, \Omega_i} \prod_i p_i^2 dp_i d\Omega_i \delta(t - \sum_{j=1,3} p_j^2/2m_j) \delta(\sum_k \vec{p}_k),$$

where t is the total energy of the three-particle system and the δ functions conserve energy and momentum. Integrating over the δ functions allows the elimination of Ω_3 , p_3 , and p_2 :

$$N_T = \int N(p_1, \Omega_1, \Omega_2) p_1^2 dp_1 d\Omega_1 d\Omega_2,$$

⁴ T. H. Berlin and G. E. Owen, Nucl. Phys. **5**, 669 (1958); Cao Xuan Chuan, J. Phys. Radium **23**, 78 (1962).

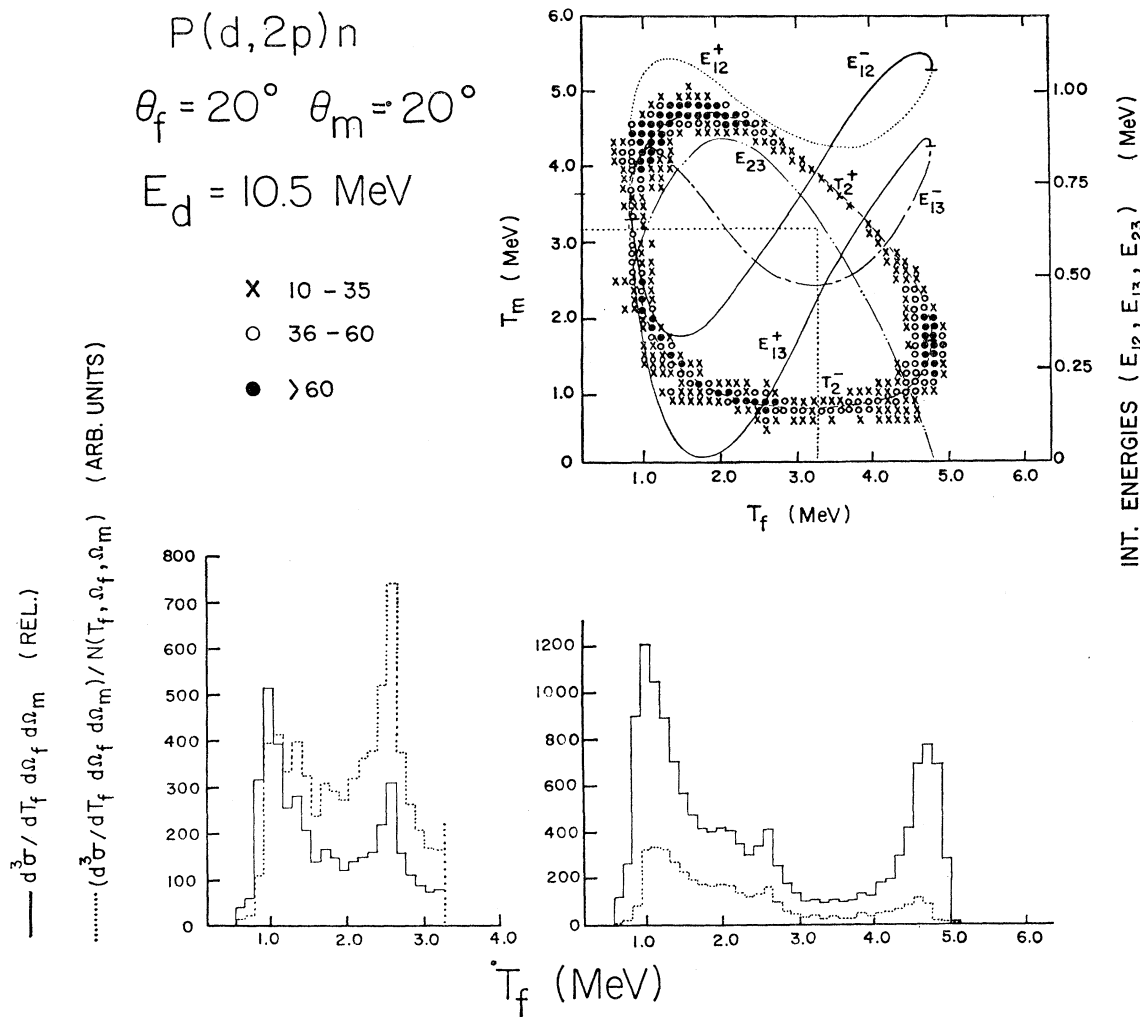


FIG. 3. A two-parameter spectrum of the ${}^4\text{H}(d, 2p)n$ reaction taken at a bombarding energy of 10.5 MeV and $\theta_f = \theta_m = 20^\circ$. The loci T_2^+ and T_2^- indicate the two possible solutions of T_2 for the corresponding value of T_f . It is noted that, for this choice of parameters, the distribution falls along a closed curve. The locus E_{23} represents values for the internal energy of the system (2, 3) if one considers the proton detected in the fixed counter (1) to be first emitted. E_{23} is single-valued for every value of T_f . The curves E_{13}^+ and E_{13}^- are the loci of values for the internal energy of the system (1, 3) when the proton detected in the movable counter (2) is considered to be first emitted. E_{13} is double-valued, with E_{13}^+ corresponding to T_2^+ solutions and E_{13}^- to T_2^- solutions. E_{12}^+ and E_{12}^- are similar loci for the internal energy of the system (1, 2) when the neutron is first emitted. The distribution along the total kinematic locus has been projected back onto the T_f axis, and is shown directly below the two-parameter presentation of the data. Also, only the lower left-hand portion of the curve, corresponding to the region of lowest excitation in the (1, 2) system, has been projected back onto the T_f axis and is shown to the left of the first projection. The dotted histograms in both cases correspond to the ratio of the yield to the appropriate available phase-space.

where

$$N(p_1, \Omega_1, \Omega_2) = \frac{m_3 p_1^2 p_2^2}{|p_2[(m_2 + m_3)/m_2] + p_1 \cos \theta_{12} - p_0 \cos \theta_2|}$$

To compare with the experimental data, the function $N(T_1, \Omega_1, \Omega_2)$ is desired:

$$N(T_1, \Omega_1, \Omega_2) = (\partial p_1 / \partial T_1) N(p_1, \Omega_1, \Omega_2) = (m_1 / p_1) N(p_1, \Omega_1, \Omega_2).$$

The numerical integration over the experimental solid angle of the function $N(T_1, \Omega_1, \Omega_2)$ yields a distribution $N(T_1)$ which can be divided out of the experimental data in order to correct for the phase-space effect in the data. An example of this is shown in Fig. 1.

IV. INTERPRETATION OF THE DATA

The major results of the data thus far collected are illustrated in Figs. 1-4. The ${}^2\text{H}(p, 2p)n$ data collected for bombarding energies of 9.0 and 10.5 MeV are dis-

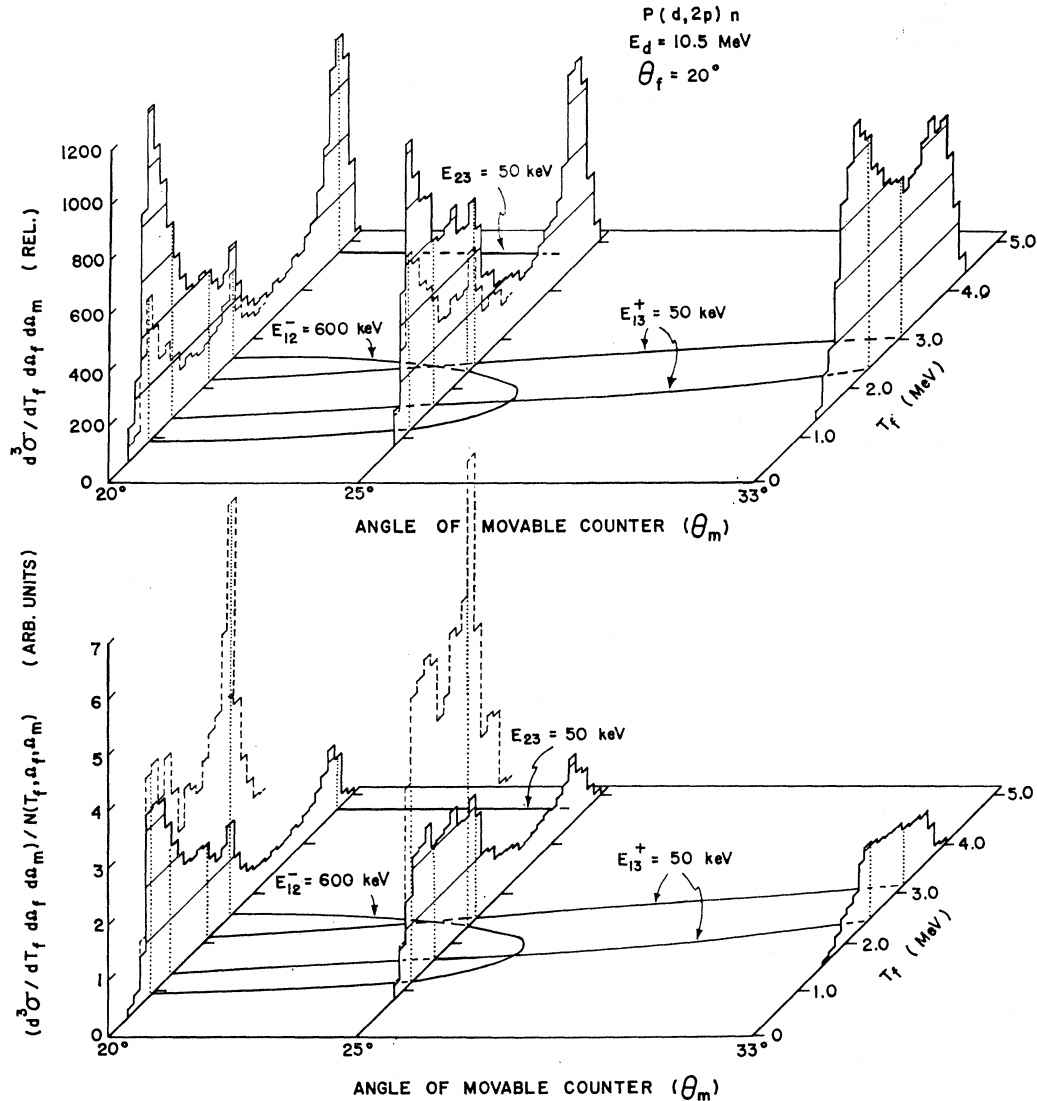


FIG. 4. A three-dimensional, isometric projection of the coincident events for the ${}^1\text{H}(d, 2p)n$ reaction in the $T_{\text{fixed}}, \theta_{\text{moving}}$ plane (see Fig. 1). The bombarding energy is 10.5 MeV and θ_{fixed} is 20° . The upper diagram consists of the collected data presented as cross section versus T_f versus θ_m , while the lower diagram is the ratio of the yield to the available phase-space. The dashed histograms correspond to the same type of projection, but only involve the lower left-hand portion of the allowed locus, as described in Fig. 3. The distribution along this portion of the curve seems to peak in each case in the region of $E_{12}^- = 600$ keV, corresponding to a di-proton system of 600 keV internal energy.

played as cross section versus T_f (the laboratory energy of the particle detected in the fixed detector) versus θ_m (the angle of the movable detector).

The internal energy curves $E_{23} = 50$ keV and $E_{13}^+ = 50$ keV (notation is explained in caption of Fig. 3) are plotted as reference curves on the data. The increased intensity in the regions of low internal energy in the (2, 3) and (1, 3) systems indicates that the reaction is proceeding largely via sequential decay through the virtual, singlet deuteron.

The data from the reaction ${}^1\text{H}(d, 2p)n$ are shown in

Figs. 3 and 4. Figure 3 illustrates the appearance of a typical spectrum, showing how the collected data fall along a locus, indicated by the T_2^+ and T_2^- loci, in the T_f, T_m plane. Additional curves are drawn on the diagram to indicate the variation of the internal energies of different intermediate systems for sequential decay. The projections of the data are explained in the figure caption.

Of particular interest is the projection of the lower portion of the kinematic locus in the region of low internal energy of the $p+p$ system. This projection is

displayed again in Fig. 4, along with similar projections of the data at two other angles. In this figure the locus of $E_{12}^- = 600$ keV has been drawn in on the T_f , T_m plane, showing a peaking of intensity in this region corresponding to a proton-proton interaction of some 600 keV. The unexpected energy and widths of the peaks perhaps indicates an interference effect, similar

to that discussed by Phillips⁵ and Bronson,³ causing the separation and narrowing of these peaks which probably correspond to a broader, lower internal energy interaction than that observed.

⁵ G. C. Phillips, *Rev. Mod. Phys.* **36**, 1085 (1964); G. C. Phillips, paper in this conference, *Rev. Mod. Phys.* **37**, 409 (1965).

$D(p, 2p)n$ Reaction at 31 MeV*

S. M. BUNCH, C. C. KIM, H. H. FORSTER

University of Southern California, Los Angeles, California

I. INTRODUCTION

Studies involving the interaction of protons with deuterons are important because of the interest in nucleon-nucleon interactions, three-body forces, and deuteron states. In addition, the fact that the deuteron is so loosely bound permits one to use certain approximations which cannot ordinarily be made in the theoretical treatment of nuclear reactions.

The nucleon-deuteron breakup problem has been formulated in the Born approximation by several investigators,¹⁻⁴ and in the impulse approximation by Chew.⁵ The direct application of either of these approaches is quite difficult; but the approximations suggested by Frank and Gammel,⁶ and Kuckes, Wilson, and Cooper⁷ can be more easily applied. The first of these relates the $D(p, 2p)n$ reaction to p - d scattering, while in the second, the neutron is treated as a spectator particle.

Experimentally, the breakup of the deuteron following proton bombardment has been investigated over a wide range of incident proton energies.^{6,8-13} However, scattering experiments involving the detection of one outgoing particle do not seem to lead to conclusive information.

* Work supported in part by the U.S. Atomic Energy Commission.

¹ T. Y. Wu and J. Ashkin, *Phys. Rev.* **73**, 986 (1948).

² G. F. Chew, *Phys. Rev.* **74**, 809 (1948).

³ F. de Hoffman, *Phys. Rev.* **78**, 216 (1950).

⁴ R. L. Gluckstern and H. A. Bethe, *Phys. Rev.* **81**, 761 (1951).

⁵ G. F. Chew, *Phys. Rev.* **80**, 196 (1950).

⁶ R. M. Frank and J. L. Gammel, *Phys. Rev.* **93**, 463 (1954).

⁷ A. F. Kuckes, R. Wilson, and P. F. Cooper, Jr., *Ann. Phys. (N. Y.)* **15**, 193 (1961).

⁸ W. H. Barkas and M. G. White, *Phys. Rev.* **56**, 288 (1939).

⁹ L. Cranberg and R. K. Smith, *Phys. Rev.* **113**, 587 (1959).

¹⁰ S. Kikuchi, J. Sanada, S. Suwa, I. Hayashi, K. Nisimura, and K. Fukunaga, *J. Phys. Soc. Japan* **15**, 749 (1960).

¹¹ K. Nisimura, *J. Phys. Soc. Japan* **16**, 2097 (1961).

¹² W. T. H. Van Oers and K. W. Brockman, *Nucl. Phys.* **47**, 338 (1963).

¹³ D. G. Stairs, R. Wilson, and P. F. Cooper, Jr., *Phys. Rev.* **129**, 1672 (1963).

Recently angular correlations of coincident protons emitted in the deuteron breakup have been studied at 18 MeV,¹⁴ 50 MeV,¹⁵ and 145 MeV.¹⁶ Of these, only the 145-MeV data agreed with the predictions of the spectator model; for the lower energy experiments the difference between the simple predictions of the model and the experimental data was considerable; nor was an analysis of the 18-MeV results with a Frank-Gammel calculation more successful.

II. EXPERIMENTAL PROCEDURE

The 31-MeV proton beam of the University of Southern California linear accelerator was used to bombard a gaseous deuterium target. The scattering chamber has previously been described in detail,¹⁶ except that it was modified by the insertion of a rotating, O-ring vacuum seal in the top through which the size of an internal collimator was controlled. Solid targets for calibration purposes could be inserted into the beam line from the bottom of the chamber.

The collimated proton beam, after leaving the end of the beam pipe which consisted of a $\frac{1}{4}$ -in.-diam nickel collimator and a 0.002-in. Al window, passed through $\frac{1}{2}$ in. of air and a 0.001-in. Al chamber window into the chamber filled with 99.5% pure deuterium gas, at a pressure of 200–600 Torr. Charge collection took place in a Faraday cup placed behind the chamber. The scattered particles were stopped and detected by 1-in. NaI(Tl) crystals mounted onto 6655A photomultiplier tubes. One scattering arm was fixed at 35° and the other was continuously variable. In the fixed scattering arm (upper arm), the particle passed through a 60- μ surface-barrier solid-state detector. The geometry was determined by $\frac{3}{4}$ -in.-diam collimators placed directly in front of the NaI(Tl) crystals. These collimators were

¹⁴ R. E. Warner, *Phys. Rev.* **132**, 2621 (1963).

¹⁵ R. J. Griffiths and K. M. Knight, *Nucl. Phys.* **54**, 56 (1964).

¹⁶ C. C. Kim, S. M. Bunch, D. W. Devins, and H. H. Forster, *Nucl. Phys.* (to be published).